



TITLE:

Inconsistency and uncertainty of the human visual area loci following surface-based registration: Probability and Entropy Maps.

AUTHOR(S):

Yamamoto, Hiroki; Fukunaga, Masaki; Takahashi, Shigeko; Mano, Hiroaki; Tanaka, Chuzo; Umeda, Masahiro; Ejima, Yoshimichi

CITATION:

Yamamoto, Hiroki ...[et al]. Inconsistency and uncertainty of the human visual area loci following surface-based registration: Probability and Entropy Maps.. Human brain mapping 2012, 33(1): 121-129

ISSUE DATE:

2012-01

URL:

<http://hdl.handle.net/2433/152357>

RIGHT:

© 2011 Wiley Periodicals, Inc.; The definitive version is available at www3.interscience.wiley.com

Hiroki Yamamoto

Inconsistency and Uncertainty of the Human Visual Area Loci following Surface-based Registration: Probability and Entropy Maps

Hiroki Yamamoto¹, Masaki Fukunaga², Shigeko Takahashi³,
Hiroaki Mano⁴, Chuzo Tanaka⁴, Masahiro Umeda², and Yoshimichi Ejima⁵

¹Department of Human Coexistence, Graduate School of Human and Environmental
Studies, Kyoto University, Kyoto, Japan

²Department of Medical Informatics,

³Faculty of Fine Arts, Kyoto City University of Arts, Kyoto, Japan
Meiji University of Oriental Medicine, Kyoto, Japan

⁴Department of Neurosurgery, Meiji University of Oriental Medicine, Kyoto, Japan

⁵Kyoto Institute of Technology, Kyoto, Japan

*Correspondence to: **Dr. Hiroki Yamamoto**

Department of Human Coexistence

Graduate School of Human and Environmental Studies, Kyoto University

Yoshida Nihonmatsu-cho, Sakyo-ku, Kyoto 606-8501, Japan

E-mail: yamamoto@cv.jinkan.kyoto-u.ac.jp

Tel: +81-75-753-2978; Fax: +81-75-753-6574

Short Title: Probability and Entropy Maps of Visual Areas

Keywords: human visual cortex, probabilistic atlas, information theory, retinotopy,
fMRI

Hiroki Yamamoto

1 **ABSTRACT**

2

3 Here we created two different multisubject maps (16 subjects) to characterize
4 interindividual variability in the positions of human visual areas (V1, dorsal and
5 ventral parts of V2/3, V3A, V3B, V7, LOc, MT+, and hV4 [or V4v and V8]), which
6 were localized using fMRI and coregistered using a surface-based method. The first
7 is a probability map representing the degree of alignment inconsistency for each area,
8 in which each point in space is associated with the probability affiliated with a given
9 area. The second, a novel map termed an entropy map in which each point is
10 associated with Shannon entropy computed from the probabilities, represents the
11 degree of uncertainty regarding the area that resides there, and is maximal when all
12 areas are equally probable. The overall average probability and entropy values were
13 about 0.27 and 1.15 bits, respectively, with dependencies on the visual areas. The
14 probability and entropy maps generated here will benefit any application which
15 requires predictions of areas that are most likely present at an anatomical point and
16 know the uncertainty associated with such predictions.

17

Hiroki Yamamoto

1 INTRODUCTION

2

3 The human visual cortex consists of multiple functionally distinct visual areas, many
4 of which have been individually localized on the cortical surface by imaging their
5 associated retinotopic activity or cytoarchitecture. Their locations can be
6 quantitatively compared among individuals once they are expressed in common
7 coordinate space by registering each individual's brain into a common standard
8 brain. Such comparisons have been made using various interindividual registration
9 methods: linear volume-based (Amunts et al., 2000; Dougherty et al., 2003; Hasnain
10 et al., 1998; Rottschy et al., 2007), nonlinear volume-based (Roland et al., 1997), and
11 surface-based methods (Fischl et al., 1999b; Hinds et al., 2008; Van Essen and Dierker,
12 2007; Van Essen et al., 2001). Since interindividual registration is widely used to
13 describe the loci of brain activation or lesions, and to normalize functional data
14 between individual brains, evaluation of interindividual variability after registration
15 is essential for reliably interpreting a broad range of brain function data.

16 Here, we propose that inconsistency and uncertainty are fundamental concepts
17 characterizing interindividual variability in the visual area loci. Inconsistency refers
18 to disparity between individuals regarding the location of a particular visual area.
19 Inconsistency in a standard space has been assessed in several studies by calculating
20 the variance of the position of a representative point within a visual area (Dougherty
21 et al., 2003; Hasnain et al., 1998), or constructing a probabilistic map in which each

Hiroki Yamamoto

1 point is associated with a probability that the visual area resides there (Amunts et al.,
2 2000; Fischl et al., 1999b; Hinds et al., 2008; Roland et al., 1997; Van Essen and
3 Dierker, 2007; Van Essen et al., 2001). While inconsistency provides a good basis for
4 analyzing a single, isolated area, it is inherently insufficient for mapping multiple
5 visual areas with pairwise adjacency. When transforming multiple areas together
6 into a standard space, their adjacency causes overlap between neighboring areas of
7 different individuals. Therefore, in evaluating interindividual variability in multiple
8 visual areas, we are inevitably faced with another problem, uncertainty.

9 Uncertainty relates to the difficulty of knowing which visual areas reside at a
10 given position; the greater the number of overlaps between different areas, the
11 greater the degree of uncertainty. It should be emphasized here that uncertainty is
12 an entirely different concept from inconsistency. Even if there is no area that has a
13 high probability of being present at an anatomical point, the uncertainty at the point
14 is zero **only if** a single area has a non-zero probability of being present. Conversely,
15 even if an area has a high probability of being present, the uncertainty is large if
16 other areas also have a high probability of being present. When an activation focus is
17 observed at such a point, we cannot confidently attribute it to any one area.
18 Additionally, when individual brain activations are pooled in a standard space,
19 caution is warranted regarding the source of activation at such points, since
20 activations of different areas are probably highly confounded. One may argue that a
21 difference in utility between entropy and probability would disappear if probability

Hiroki Yamamoto

1 was sufficiently high. Yet this is not the case, as we shall see in the Results section.
2 These considerations suggest that quantification of uncertainty is crucial for reliably
3 interpreting functional data after interindividual registration. However, this issue
4 has not been investigated.

5 In the present study, we developed a probabilistic and information theoretic
6 framework to quantify uncertainty as well as inconsistency, and used this
7 framework to analyze multiple human visual areas which were localized based on
8 functional MRI (fMRI) retinotopy measurements. Inconsistency was estimated by
9 generating a probability map based on the data from 16 subjects that had been
10 coregistered by a surface-based method (Fischl et al., 1999b), in which each point
11 was associated with a probability that it belonged to each retinotopic area. We used
12 Shannon entropy (Shannon, 1948) as a measure of uncertainty to generate a novel
13 map we called an entropy map, where each point was associated with an entropy
14 value computed from the probability that the point belongs to each of the visual
15 areas.

Hiroki Yamamoto

1 METHODS

2

3 Quantification of the inconsistency and uncertainty of the locations of human
4 retinotopic areas are comprised of three basic steps: 1) localization of retinotopic
5 areas on individual cortical surfaces using fMRI, 2) generation of the probability
6 map using a surface-based registration, and 3) generation of the entropy map. Unless
7 otherwise mentioned, the analyses were performed and visualized using in-house
8 software written in VTK/ITK (Kitware, Clifton Park, NY) and MATLAB (Mathworks,
9 Natick, MA), which has been successfully applied to the cortical surface-based
10 analysis of fMRI data (Ban et al., 2006; Ejima et al., 2003).

11

12 *Localizations of Retinotopic Areas using fMRI*

13 *Subjects.* We studied 32 hemispheres from 16 normal subjects (2 female, 14 males;
14 ages 22-59 years, mean 29 years). Subjects were in good health with no past history
15 of psychiatric or neurological disease. All but one subject was strongly right-handed.
16 The study protocols were approved by the Human Studies Committee of the
17 Graduate School of Human and Environmental Studies at Kyoto University and the
18 Department of Neurosurgery at Meiji University of Oriental Medicine. All subjects
19 provided written informed consent prior to study enrolment.

20 *Imaging methods.* The imaging apparatus and methods have been described in
21 detail elsewhere (Yamamoto et al., 2008). Briefly, structural and functional MRI

Hiroki Yamamoto

measurements were carried out using a standard clinical 1.5 Tesla scanner (General Electric Signa NV/i, Milwaukee, WI). Prior to experimental scans, high-contrast T1-weighted structural images of the whole brain were recorded for each subject, which were used for reconstructing the individual brain surface. For each subject, three types of images were obtained on each scanning session, with a standard flexible surface coil placed at the occipital pole. First, T1-weighted structural images were acquired for anatomical registration. Second, a set of 16 or 17 adjacent high-resolution T1-weighted anatomical slices was obtained. Finally, multiple functional scans were obtained in the same slices as these anatomical slices while the subject viewed visual stimuli, using a T2*-weighted two-dimensional gradient echo, echo planar imaging.

Retinotopic mapping of visual areas. After reconstructing each individual's cortical surface, the locations of retinotopic visual areas (V1, V2d, V3d, V3B, V3A, V7, LOc, MT+, V2v, V3v, hV4, V4v, and V8) were identified based on fMRI data using standard retinotopic mapping procedures. **Since the organization of visual areas in the ventral occipital cortex remains controversial, we adopted two different parcellation schemes in this region: one consisting of V4v and V8 (Hadjikhani et al., 1998), referred to as the V4v/V8 model, while the other of just hV4 (Winawer et al., 2010), called the hV4 model. We created probability and entropy maps for each model (for details see Supplemental Methods and Supplemental Fig. S1). Details of the surface mapping procedures have been described elsewhere (Yamamoto et al.,**

Hiroki Yamamoto

2008) and outlined in **the** Supplemental Methods. The parcellation of the areas led to a cortical surface for each subject's hemisphere, each vertex of which had an integer label that specified which areas **reside** there.

Estimating Inconsistency: Generation of the Probability Map

Surface-based registration. The labeled cortical surfaces were registered to the FreeSurfer average template surface, using Automated Spherical Warping (Fischl et al., 1999b) of the FreeSurfer software package (Dale et al., 1999; Fischl et al., 1999a) which displaced the vertices of each labeled surface so as to match its folding pattern with that of the template. This intersubject registration was performed separately for the groups of left and right hemispheres.

Generation of the probability map. The probability of the occurrence of each area on the template surface was computed by counting the number of overlaps of the area's label in different hemispheres and dividing this by the total number of samples ($n = 16$) for each left or right hemisphere. This computation was repeated at every vertex of the template surface, thus yielding a probability surface map for each retinotopic area (Fig. 1A). Furthermore, the probability maps for all the retinotopic areas were integrated into a maximum probability map (Fig. 1B), where each vertex was assigned a label indicating which area had the greatest probability of being present there and was then given the maximum value.

Hiroki Yamamoto

[Figure 1 about here]

Estimating Uncertainty: Generation of the Entropy Map

To estimate the uncertainty regarding which of the retinotopic areas is located on the template surface, we introduced Shannon entropy (Shannon, 1948). The Shannon entropy (H) of the retinotopic areas can be expressed in terms of the probabilities (p_i) of the different retinotopic areas, and given by

$$H = - \sum_{i=1}^n p_i \cdot \log_2 p_i [\text{bits}], \quad (1)$$

where n is the total number of candidate areas. By applying this equation to the probability maps of retinotopic areas, we calculated the entropy for each vertex on the template surface (Fig. 1C). In the present analysis, **$n = 12$ for hV4 model or 13 for V4v/V8 model; the probability of each retinotopic area $p_1, p_2, \dots, p_{11(12)}, p_{12(13)}$; none of them, $p_{12(13)}$. Thus, the upper limit of entropy is $\log_2 12(13) \cong 3.6(3.7)$ bits, which occurs when we are completely uncertain about which of the 12(13) events happens at a certain vertex; in other words, when we have no prior knowledge of the area's cortical organization.**

Hiroki Yamamoto

1

2 RESULTS

3 We created surface-based probability and entropy maps of the visual areas, where
4 each vertex was associated with occurrence probabilities ($n = 16$) for each of the areas
5 and entropy of the probability distribution, respectively. The maps are publicly
6 available in FreeSurfer and VTK file formats (Supplementary material online at
7 <http://hbm.s3.amazonaws.com/ProbabilityMap.zip>). One can use them to explore the
8 maps in 3D space and inspect the data for a particular vertex of the FreeSurfer
9 average surface in MNI coordinate space, in conjunction with freeware surface
10 viewers (such as tksurfer and ParaView). The essence of the data is presented in Fig.
11 2, which shows the maximum probability map (A, C) and the entropy map (B, D)
12 overlaid on the FreeSurfer average left and right hemispheres **for each of the two**
13 **models of visual area organization: V4v/V8 and hV4.**

14

15 [Figure 2 about here]

16

17 *Inconsistency in the Locations of Visual Areas: Probability Map*

18 The maximum probability area changes on the surface in the hierarchical order (Fig.
19 2AC). However, the probabilistic volume for a corresponding area was not
20 definitively circumscribed (e.g., see Fig. 1A for V1, V2v, and V3v). This positional
21 inconsistency was analyzed for individual visual areas by averaging all the

Hiroki Yamamoto

probability values over each probabilistic area on both hemispheres (vertices containing non-zero probability). The average probability is compared among the visual areas of **V4v/V8 model** in Fig. 3A. The average probability was somewhat different among areas with the largest value for V1, indicating the lowest alignment inconsistency. The reproducibility of the areal difference was tested by splitting all samples into left and right hemispheres, and further splitting subjects into two subgroups within each hemisphere. These data sets were then analyzed independently. The parallel coordinates plot of the results (Fig. 3B) clearly shows that the areal difference is highly reproducible. The correlation coefficients between different hemispheres were 0.730 ($p = 7.1 \times 10^{-3}$), and those between different subgroups were 0.844 ($p = 5.5 \times 10^{-4}$) for the left hemisphere and 0.941 ($p = 5.1 \times 10^{-6}$) for the right hemisphere. The average probability over the 12 retinotopic areas was 0.274 (SD: 0.074). **We also applied similar analyses as described above to the hV4 model map and obtained essentially similar results (Supplemental Fig. S2).**

[Figure 3 about here]

Uncertainty in the Locations of Visual Areas: Entropy Map

The average entropy is compared across the areas of **the V4v/V8 model** in Fig. 4A. According to the size of average entropy, visual areas were grouped into three classes: 1) V3d and V3B with higher values (~ 1.5 bits), 2) V1, V7, V8, and MT+ with

Hiroki Yamamoto

lower values (< 1.0 bits), and 3) the other areas with intermediate values. Although the difference appears to be small, the reproducibility of the difference was confirmed by split data analyses that were similar to the analyses for the average probabilities. **It is clearly demonstrated in Fig. 4B that the three groups virtually remained even when data were split into different hemisphere and subject samples.** The exception was V3v, which had higher values comparable to V3d and V3B only for the left hemisphere. The areal dependency was highly correlated between hemispheres ($r = 0.955$, $p = 1.3 \times 10^{-6}$) and different subject samples ($r = 0.913$, $p = 3.5 \times 10^{-5}$ for the left hemisphere; $r = 0.915$, $p = 3.0 \times 10^{-5}$ for the right). The average entropy over the 12 visual areas was 1.15 bits (SD: 0.2).

[Figure 4 about here]

Entropy is conceptually and computationally distinct from maximum probability. However, one would argue that high entropy might be generally associated with the low probability of belonging to a given area. We examined a relationship between entropy and maximum probability on a vertex by vertex basis, but found no consistent correlation between them throughout their range (Fig. 4C). Although the expected negative correlation is observed for higher maximum probability levels (0.6–1.0), the number of vertices in the range occupies only 28.4% of all the vertices containing nonzero probability. The entropies of the vertices with lower probability levels (71.6%) disperse widely and show rather positive correlations with maximum probabilities. Notably, relatively wide dispersion remains even for the higher

Hiroki Yamamoto

1 probability levels in the negative correlation zone. Consequently, entropy provides
2 information distinct from that conveyed by maximum probability, indicating the
3 importance of the entropy map. **We also applied similar analyses as above to the**
4 **hV4 model map and obtained essentially the same results (Supplemental Fig. S3).**
5

Hiroki Yamamoto

1

2 DISCUSSION

3

4 *Inconsistency in the Locations of Visual Areas: Probability Map*

5 In the present study, the alignment inconsistency of retinotopic areas was analyzed
6 using a probabilistic approach (Mazziotta et al., 1995; Roland and Zilles, 1994). Such
7 analyses have been made for cytoarchitectonic definitions of areas V1 and V2 in five
8 (Roland et al., 1997) and 10 brains (Amunts et al., 2000), and areas V3v and V4v in
9 ten brains (Rottschy et al., 2007), all of which had been coregistered using
10 volume-based methods. The cytoarchitectonic studies on V1 and V2 have
11 demonstrated that the probability volume of V2 surrounds that of V1 with
12 substantial overlap, implying that the inconsistency is large, but not so large as to
13 grossly violate the positional relationship. This observation has been extended by
14 Van Essen *et al.* (2001) to multiple visual areas identified using fMRI for four
15 hemispheres in conjunction with a surface-based registration. Our study has
16 revealed the moderate inconsistencies in the probability maps by collecting larger
17 samples in conjunction with a surface-based registration.

18 Regarding the comparisons across areas, it has been noted that the degree of
19 inconsistency is smaller for V1 than V2 in cytoarchitectonic studies (Amunts et al.,
20 2000). There is agreement between the anatomical and functional probability maps
21 reported for areas V1 and V2 (Wohlschlager et al., 2005). The present fMRI study

Hiroki Yamamoto

quantitatively confirmed this by introducing a measure of average probability. The average probability of our functionally defined V1 was ~ 0.5 , which was comparable or slightly smaller than that of cytoarchitectonically defined V1 coregistered with the identical surface-based method to ours (Hinds et al., 2008). This is somewhat surprising because the higher accuracy of cytoarchitectonic map is considered to yield higher probabilities, and in turn suggests high accuracy of functional segmentation of retinotopic areas. Furthermore, the average probability showed a subtle, but reproducible, variation among multiple visual areas. The grand average across all areas was found to be only ~ 0.3 , indicating substantial inconsistency.

Uncertainty in the Locations of Visual Areas: Entropy Map

The application of Shannon entropy to individual brain variability is a novel aspect of the present study. It should be stressed that even if events are highly probable, entropy is large when the different events occur simultaneously, that is, when the different areas overlap one another. Herein **lays** the significance of the entropy map. Indeed, our analysis of the relationship between the entropy and maximum probability maps (Fig. 4C) revealed that these statistics were largely unrelated, empirically supporting the dissociation between them for human visual areas. Although the dissociation has not been explicitly examined, the overlap between different structures has been noted in the context of brain registration. Roland *et al.* (1997) identified areas V1 and V2 cytoarchitectonically and reported

Hiroki Yamamoto

that the overlap between V1 and V2 is as large as the overlap between V1 areas of different brains. Van Essen (2005) analyzed the degree of overlap between neighboring brain sulci using a probability map. These studies all disregarded the occurrence probabilities of overlapping structures, notwithstanding the fact that the uncertainty is maximal when each event is equiprobable. The present study further deepened our understanding of uncertainty in interindividual registration by employing the concept of entropy.

We found that the surface-based registration brought the overall average entropy of retinotopic areas to approximately 1 bit, indicating that there is on average 1 bit of uncertainty about which the retinotopic area was present at a point on the cortical surface. In addition, we found that there was also a mild, but highly reproducible, variation in entropy among retinotopic areas.

Applications and Caveats

The present probabilistic and information theoretical framework is useful for a variety of applications related to interindividual variability in the human brain. Probability and entropy maps of retinotopic areas can be beneficial for any application that predicts which areas are present with high probability at an anatomical point, and to know the uncertainty associated with that prediction. Using these maps, researchers and clinicians can identify, with a known degree of uncertainty, the visual area that is most probably at an activation site or a lesion site

Hiroki Yamamoto

1 within a target brain for which any form of direct identification is impossible. The
2 other main application is in the field of brain registration and brain warping (Toga,
3 1999). As demonstrated here, the surface-based registration brings the visual area
4 entropy to about 1 bit. The performance of various registration methods can be
5 compared quantitatively using the entropy of the coregistered structures. Finally, the
6 present work on visual areas can be generalized to not only other functional
7 structures, but also other anatomical structures. Thus, an important direction of
8 future research is to extend the present framework to issues of brain
9 structure-function relationships, i.e., the focus of an ongoing large-scale international
10 project that aims to develop a probabilistic brain atlas representing many types of
11 brain function and structure (Mazziotta et al., 2001).

12 Several caveats should be heeded when one uses these probability and entropy
13 maps, or evaluates the data obtained in our analyses. First, although the sample size
14 ($n=16$) of our maps is larger than previous studies (Amunts et al., 2000; Hinds et al.,
15 2008; Rottschy et al., 2007; Van Essen et al., 2001; Wohlschlager et al., 2005), it is still
16 limited. Second, the fact that our sample was composed primarily of men would
17 have an effect on the quantified results. Finally, our functional parcellation of the
18 visual cortex is not complete. Each area localized here might be a portion of the
19 whole area, because they have an extended region representing more peripheral
20 visual field locations ($> 16^\circ$) than those measured. Thus, intersubject variability in
21 the retinotopic representation would have introduced extra variability in the

Hiroki Yamamoto

- 1 observed locations of visual areas, independent of anatomical variability.

Hiroki Yamamoto

1 CONCLUSION

2 This study provides a novel method for analyzing interindividual variability in the
3 loci of functional cortical areas. In contrast to previous approaches, which only
4 analyze the variability separately for each distinct area (called inconsistency here),
5 our approach takes into account an additional new measure of uncertainty about the
6 set of areas using entropy. The application of our method to human retinotopic
7 visual areas reveals that entropy provides information distinct from that conveyed
8 by probability, demonstrating the efficacy of our method. The importance of the
9 entropy measure will increase as divisions of cortex proceed further, thereby the
10 overlapping among registered areas will also increase.

11

Hiroki Yamamoto

1 ACKNOWLEDGEMENTS

2

3 This work was supported by the Strategic Information and Communications R&D

4 Promotion Programme of MIC, Japan., Grant-in-Aid for Young Scientists (B) and

5 Scientific Research (C), MEXT, Japan, the Global COE Program "Revitalizing

6 Education for Dynamic Hearts and Minds," MEXT, Japan, and a research grant from

7 Tateisi Science and Technology Foundation.

Hiroki Yamamoto

1 REFERENCES

- Amunts K, Malikovic A, Mohlberg H, Schormann T, Zilles K. (2000): Brodmann's areas 17 and 18 brought into stereotaxic space-where and how variable? *Neuroimage* 11(1):66-84.
- Ban H, Yamamoto H, Fukunaga M, Nakagoshi A, Umeda M, Tanaka C, Ejima Y. (2006): Toward a common circle: interhemispheric contextual modulation in human early visual areas. *J Neurosci* 26(34):8804-9.
- Dale AM, Fischl B, Sereno MI. (1999): Cortical surface-based analysis. I. Segmentation and surface reconstruction. *Neuroimage* 9(2):179.
- Dougherty RF, Koch VM, Brewer AA, Fischer B, Modersitzki J, Wandell BA. (2003): Visual field representations and locations of visual areas V1/2/3 in human visual cortex. *J Vis* 3(10):586-98.
- Ejima Y, Takahashi S, Yamamoto H, Fukunaga M, Tanaka C, Ebisu T, Umeda M. (2003): Interindividual and interspecies variations of the extrastriate visual cortex. *Neuroreport* 14(12):1579-83.
- Fischl B, Sereno MI, Dale AM. (1999a): Cortical surface-based analysis. II: Inflation, flattening, and a surface-based coordinate system. *Neuroimage* 9(2):195-207.
- Fischl B, Sereno MI, Tootell RB, Dale AM. (1999b): High-resolution intersubject averaging and a coordinate system for the cortical surface. *Hum Brain Mapp* 8(4):272-84.
- Hadjikhani N, Liu AK, Dale AM, Cavanagh P, Tootell RB. (1998): Retinotopy and color sensitivity in human visual cortical area V8. *Nat Neurosci* 1(3):235-41.
- Hasnain MK, Fox PT, Woldorff MG. (1998): Intersubject variability of functional areas in the human visual cortex. *Hum Brain Mapp* 6(4):301-15.
- Hinds OP, Rajendran N, Polimeni JR, Augustinack JC, Wiggins G, Wald LL, Diana Rosas H, Potthast A, Schwartz EL, Fischl B. (2008): Accurate prediction of V1 location from cortical folds in a surface coordinate system. *Neuroimage* 39(4):1585-99.
- Mazziotta J, Toga A, Evans A, Fox P, Lancaster J, Zilles K, Woods R, Paus T, Simpson G, Pike B, Holmes C, Collins L, Thompson P, MacDonald D, Iacoboni M, Schormann T, Amunts K, Palomero-Gallagher N, Geyer S, Parsons L, Narr K, Kabani N, Le Goualher G, Boomsma D, Cannon T, Kawashima R, Mazoyer B. (2001): A probabilistic atlas and reference system for the human brain: International Consortium for Brain Mapping (ICBM). *Philos Trans R Soc Lond B Biol Sci* 356(1412):1293-322.
- Mazziotta JC, Toga AW, Evans A, Fox P, Lancaster J. (1995): A probabilistic atlas of the human brain: theory and rationale for its development. The International Consortium for Brain Mapping (ICBM). *Neuroimage* 2(2):89-101.
- Roland PE, Geyer S, Amunts K, Schormann T, Schleicher A, Malikovic A, Zilles K.

Hiroki Yamamoto

- 1 (1997): Cytoarchitectural maps of the human brain in standard anatomical
- 2 space. *Human Brain Mapping* 5(4):222-227.
- 3 Roland PE, Zilles K. (1994): Brain atlases--a new research tool. *Trends Neurosci*
- 4 17(11):458-67.
- 5 Rottschy C, Eickhoff SB, Schleicher A, Mohlberg H, Kujovic M, Zilles K, Amunts K.
- 6 (2007): Ventral visual cortex in humans: Cytoarchitectonic mapping of two
- 7 extrastriate areas. *Hum Brain Mapp*.
- 8 Shannon CE. (1948): The mathematical theory of communication, I and II. *Bell*
- 9 *System technical journal* 27:379-443.
- 10 Toga AW. (1999): *Brain warping*. San Diego: Academic Press. xiii, 385 p. p.
- 11 Van Essen DC. (2005): A Population-Average, Landmark- and Surface-based (PALS)
- 12 atlas of human cerebral cortex. *Neuroimage* 28(3):635-62.
- 13 Van Essen DC, Dierker DL. (2007): Surface-based and probabilistic atlases of primate
- 14 cerebral cortex. *Neuron* 56(2):209-25.
- 15 Van Essen DC, Lewis JW, Drury HA, Hadjikhani N, Tootell RB, Bakircioglu M,
- 16 Miller MI. (2001): Mapping visual cortex in monkeys and humans using
- 17 surface-based atlases. *Vision Res* 41(10-11):1359-78.
- 18 Winawer J, Horiguchi H, Sayres RA, Amano K, Wandell BA. (2010): Mapping hV4
- 19 and ventral occipital cortex: the venous eclipse. *J Vis* 10.
- 20 Wohlschlager AM, Specht K, Lie C, Mohlberg H, Wohlschlager A, Bente K, Pietrzyk
- 21 U, Stocker T, Zilles K, Amunts K, Fink GR. (2005): Linking retinotopic fMRI
- 22 mapping and anatomical probability maps of human occipital areas V1 and
- 23 V2. *Neuroimage* 26(1):73-82.
- 24 Yamamoto H, Ban H, Fukunaga M, Umeda M, Tanaka C, Ejima Y. (2008): Large- and
- 25 Small-Scale Functional Organization of Visual Field Representation in the
- 26 Human Visual Cortex. In: Portocello TA, Velloti RB, editors. *Visual Cortex:*
- 27 *New Research*. New York: Nova Science Publisher. p 195-226.
- 28

Hiroki Yamamoto

FIGURE LEGENDS

Figure 1. A probabilistic and information-theoretic framework for analyzing interindividual variability in the human retinotopic area loci. **This framework was applied independently to two models of the organization of visual areas, which are different in the parcellation of the ventral occipital cortex: one consists of visual areas V4v and V8, and another consists of a single area, hV4, instead. The difference in these parcellation schemas is described in Supplemental Methods and exemplified in Supplemental Figure S1.** (A) Probabilistic maps of V1, V2v, and V3v, etc. from 16 subjects in medial views of the inflated FreeSurfer average right hemisphere. The probability that each area is located at each surface vertex is represented by a color code, as shown by the color bar. (B) The same view of the maximum probability map. The most probable visual area and its occurrence probability ($n = 16$) for each surface vertex are color-coded using different colors and brightness levels, respectively, as indicated by the color bar. (C) The same view of the entropy map. The entropy at each vertex is color-coded, as shown by the color bar.

Hiroki Yamamoto

1 Figure 2. Surface maps showing the probability or entropy of human retinotopic
2 areas after surface-based registration. **A and B show the maps for the V4v/V8 model,**
3 **while C and D show the maps for the hV4 model (see Supplemental Method and**
4 **Fig. S1 for the difference of these models).** (A, C) The maximum probability map of
5 the areas on the spherical FreeSurfer average left hemisphere is shown in the left
6 panel, and oblique lateral, ventral, and oblique medial views of the inflated surface
7 are shown sideways. The maximum probability map on the right FreeSurfer average
8 hemisphere is shown in the right panel in the same way as the left hemisphere. The
9 most probable visual area and the probability ($n = 16$) are color-coded, as shown in
10 the color bar. (B, D) The entropy map is shown in the same layout as in A. Thin lines
11 are the traces of the areal boundaries in A. The entropy is color-coded, as illustrated
12 by the color bar.

13

Hiroki Yamamoto

1 Figure 3. Inconsistency in the locations of the visual areas among different
2 hemispheres after surface-based registration. **This figure shows the data for model**
3 **V4v/V8; the data for model hV4 is presented in Supplemental Figure S2. (A)**
4 Average probability for each visual area. Error bars denote SD. (B) A parallel
5 coordinates plot of the average probability for visual areas (connected lines)
6 estimated under different sample conditions. The data for the left and right
7 hemispheres are shown on the left and right, respectively. For both of the data sets,
8 shown from center to outside are sample conditions of all 16 subjects, half-split
9 random samples-A of subjects, and half-split random samples-B.

Hiroki Yamamoto

1 Figure 4. Uncertainty regarding which visual area is located at each anatomical point
2 after surface-based registration. **This figure shows the data for model V4v/V8. The**
3 **data for model hV4 is presented in Supplemental Figure S3.** (A) Average entropy
4 of each visual area across all the area's voxels. Error bars denote SD. (B) A parallel
5 coordinates plot of the average entropy for visual areas (connected lines) estimated
6 under different sample conditions. Other details **are** as in Fig. 3B. (C)
7 Two-dimensional histogram of entropy vs. maximum probability for all the area
8 voxels. The brighter the bin, the greater the number of vertices in that range, as
9 shown by the color bar.

SUPPLEMENTAL METHODS

Retinotopic mapping of visual areas.

The surface regions delineating areas V1, V2d, V3d, V3B, V3A, V7, LOc, MT+, V2v, V3v, and hV4 [or V4v and V8] were determined by phase-encoded retinotopic mapping methods (Supplemental Fig. S1A-I, L). Two additional series of fMRI experiments were conducted to determine localization more accurately. First, foveal and peripheral representations were localized (Fig. S1J, M) using the block design in which foveal and peripheral (16°) dot stimuli were presented. Second, motion-sensitive regions were localized (Fig. S1K, N) using the block design in which expanding motion of a low contrast concentric grating was presented. The statistical significance of these activities was determined by the Fourier F-test ($p < 0.001$) (Brockwell and Davis, 1991).

We parcellated the visual cortex into 12 or 13 retinotopic areas, such that each represents a consistent retinotopic map. The polar angle map allowed us to reliably identify the borders V1/V2v(d), V2v(d)/V3v(d), V3d/V3A, and V3A/V7 as reversals in the polar angle and field sign map (Fig. S1A, C, E, G, I, L). As in other studies (for a review see Wandell et al., 2005), the borders of other visual areas were placed with less accuracy as their angle maps were not clear. We designated the region just anterior to V3d as V3B (Smith et al., 1998), whose peripheral representation seemed to be located just inferior to the V3A foveal

1 representation. We identified a region within the dorsal posterior limb of the
2 inferior temporal sulcus as MT+, which had a crude eccentricity map with a
3 predominance of foveal representation inferiorly and peripheral representation
4 superiorly (Huk et al., 2002). We confirmed that this region mostly overlapped
5 with the middle temporal region, showing a strong response to motion stimuli
6 (Fig. S1K, N). We refer to the large fan-shaped region between areas V3B and
7 MT+ as LOc (Malach et al., 1995), which had a relatively clear eccentricity
8 representation in the superior anterior direction from the confluent foveal
9 representation (Levy et al., 2001). There is an ongoing debate regarding the
10 subdivision of the ventral occipital cortex anterior to V3v. Thus, we adopted
11 two different parcellation schemes in this region: the V4v/V8 and hV4 models.
12 In the V4v/V8 model we identified two areas, V4v and V8, consistent with
13 Hadjikhani *et al.* (1998), stressing consistency in the eccentricity map
14 (Supplemental Fig. S1 F, H). In the hV4 model, we identified a single area, hV4
15 (human V4), as per Winawer *et al.* (2010), stressing consistency in the angle map
16 of our data (Supplemental Fig. S1B, D). Area V8 roughly corresponds to the
17 anterior part of hV4 (human V4) and posterior part of VO (ventral occipital)
18 (Wade et al., 2002), whereas area V4v roughly corresponded to the posterior
19 half of hV4 (Zeki et al., 1991).

20

REFERENCES

- Brockwell PJ, Davis RA. (1991): Time series: theory and methods. New York: Springer-Verlag. 577 p.
- Hadjikhani N, Liu AK, Dale AM, Cavanagh P, Tootell RB. (1998): Retinotopy and color sensitivity in human visual cortical area V8. *Nat Neurosci* 1(3):235-41.
- Huk AC, Dougherty RF, Heeger DJ. (2002): Retinotopy and functional subdivision of human areas MT and MST. *J Neurosci* 22(16):7195-205.
- Levy I, Hasson U, Avidan G, Hendler T, Malach R. (2001): Center-periphery organization of human object areas. *Nat Neurosci* 4(5):533-9.
- Malach R, Reppas JB, Benson RR, Kwong KK, Jiang H, Kennedy WA, Ledden PJ, Brady TJ, Rosen BR, Tootell RB. (1995): Object-related activity revealed by functional magnetic resonance imaging in human occipital cortex. *Proc Natl Acad Sci U S A* 92(18):8135-9.
- Smith AT, Greenlee MW, Singh KD, Kraemer FM, Hennig J. (1998): The processing of first- and second-order motion in human visual cortex assessed by functional magnetic resonance imaging (fMRI). *J Neurosci* 18(10):3816-30.
- Wade AR, Brewer AA, Rieger JW, Wandell BA. (2002): Functional measurements of human ventral occipital cortex: retinotopy and colour. *Philos Trans R Soc Lond B Biol Sci* 357(1424):963-73.
- Wandell BA, Brewer AA, Dougherty RF. (2005): Visual field map clusters in human cortex. *Philos Trans R Soc Lond B Biol Sci* 360(1456):693-707.
- Winawer J, Horiguchi H, Sayres RA, Amano K, Wandell BA. (2010): Mapping hV4 and ventral occipital cortex: the venous eclipse. *J Vis* 10.
- Zeki S, Watson JD, Lueck CJ, Friston KJ, Kennard C, Frackowiak RS. (1991): A direct demonstration of functional specialization in human visual cortex. *J Neurosci* 11(3):641-9.

SUPPLEMENTAL FIGURE LEGENDS

Supplemental Figure S1. Locations of retinotopic areas, V1d/v, V2d/v, V3d/v, V3A, V3B, V7, hV4, V4v, V8, LOc, and MT+, in one subject's (S1) hemispheres and their relationship to visual field representation (up to 16° eccentricities), and motion-responsive regions of the visual cortex. Data on the left and right hemispheres are shown in the left and right regions of the figure, respectively. The colored lines on the inflated cortices indicate each area's border by the color code below A and B. Note the overlap of hV4, V4v, and V8 in the ventral occipital cortex. We adopted two different parcellation schemes in this region: one consisting of V4v and V8, the other is hV4 alone. We created probability and entropy maps independently for each schema. (A, B, C, and D) Angular visual field representation measured by the phase-encoding retinotopy experiment. A and C display the entire data of the visual cortex, while B and D zoom in on the posterior ventral region to better visualize the angular representation near areas hV4, V4v and V8. The color overlay on the cortex indicates the preferred stimulus angle at each cortical point by the color code to the right of A or C. The more saturated the color, the higher the statistical significance of retinotopic activity, as shown in the rainbow-like color bar. (E, F, G, and H) Eccentricity visual field representation measured by the phase-encoding retinotopy experiment. The data is presented in the same

1 format as A, B, C, and D. (I and L) Field sign map computed from the angular
2 and eccentricity maps. The blue code indicates mirror-image representation,
3 while the yellow indicates non-mirror-image representation. The more the color
4 is saturated, the stronger the degree of the mirror- or non-mirror-image (see the
5 color bar on the bottom). (J and M) Foveal or peripheral representation
6 measured by the experiment using the standard block paradigm. The yellow
7 region indicates fMRI activity evoked by foveal stimulation, while the blue
8 indicates activity by peripheral (16°) stimulation (see the color bar at the
9 bottom). (K and N) Motion-sensitive regions. The yellow region indicates fMRI
10 activity evoked by the expanding motion of a low contrast concentric grating
11 (see the color bar at the bottom).

12

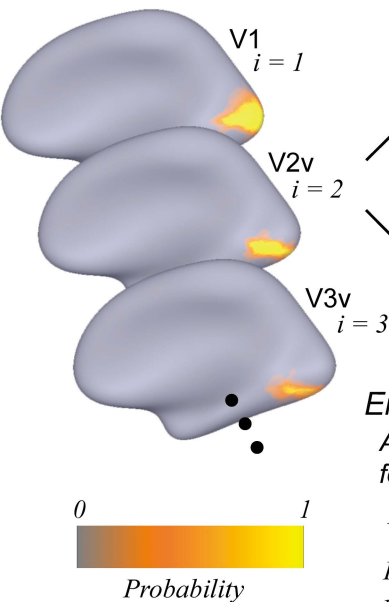
1 Supplemental Figure S2. Inconsistency in the locations of the visual areas
2 among different hemispheres after surface-based registration. This figure shows
3 the data for the hV4 model. Other details are consistent with those in Fig. 3. The
4 average probability over the 11 retinotopic areas was 0.279 (SD: 0.074).

5

1 Supplemental Figure S3. Uncertainty regarding which visual area is located at
2 each anatomical point after surface-based registration. This figure shows the
3 data for the hV4 model. Other details are consistent with those in Fig. 4. The
4 average entropy over the 11 visual areas was 1.14 bits (SD: 0.2).

5

A



MAX Operation

Entropy Computation
Applying Shannon Formula
for each surface node

$$H = - \sum_{i=1}^n p_i \cdot \log p_i$$

H : entropy [bits]

p_i : probability of i -th area

n : total number of areas (12 or 11)

Probability
0 1



C

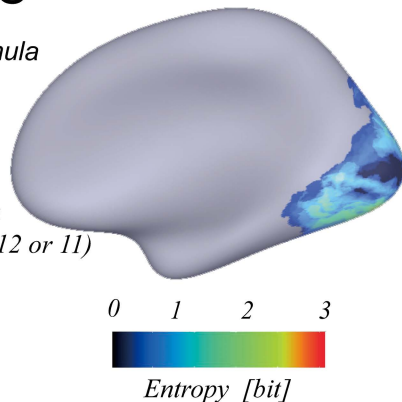
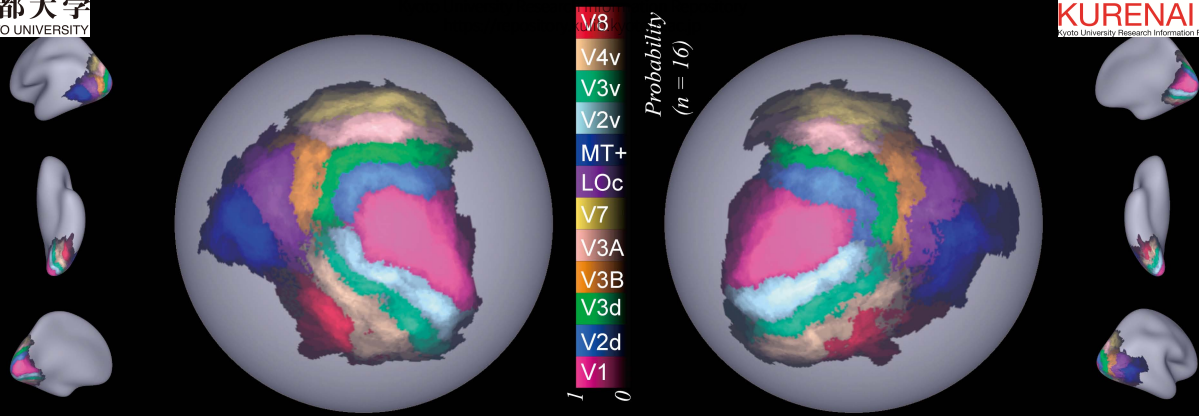
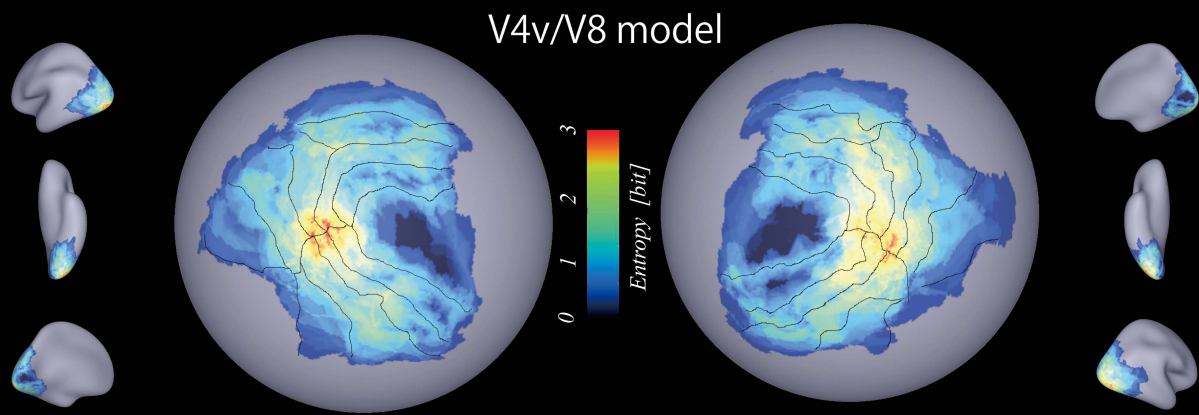


Figure 1.

A



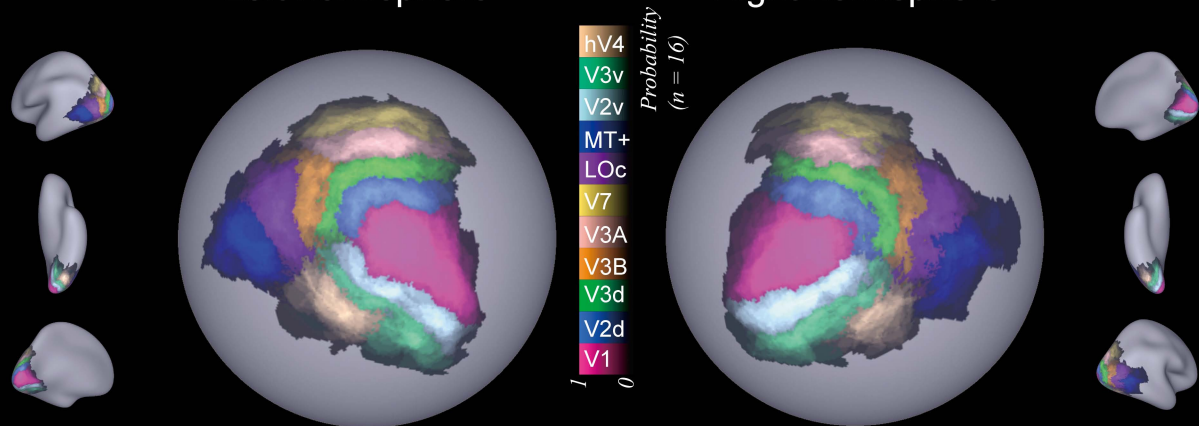
B



Left hemisphere

Right hemisphere

C



D

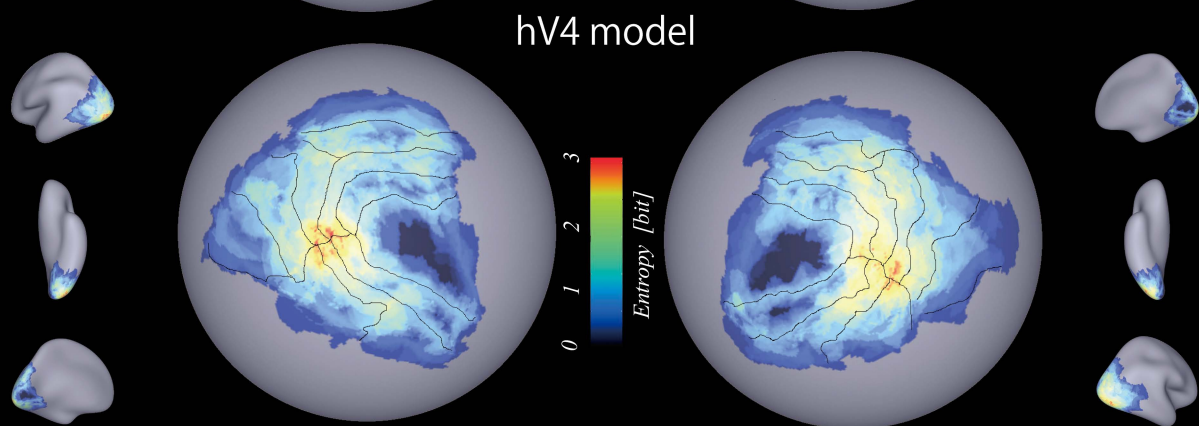


Figure 2.

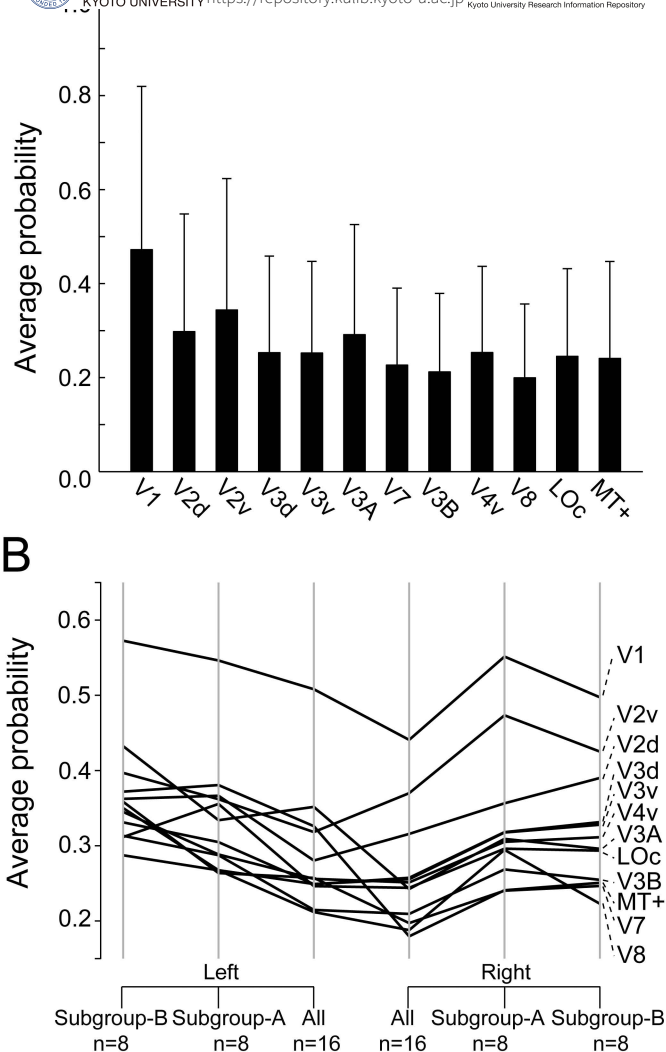
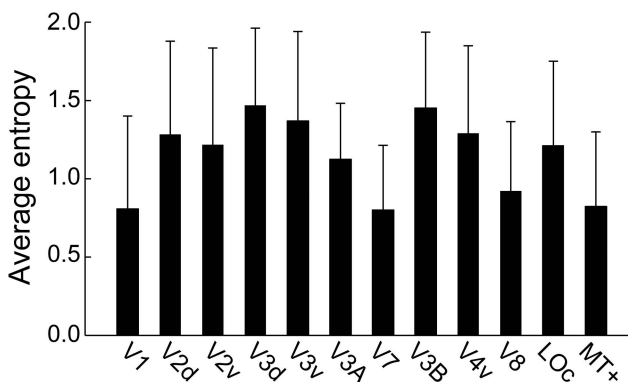
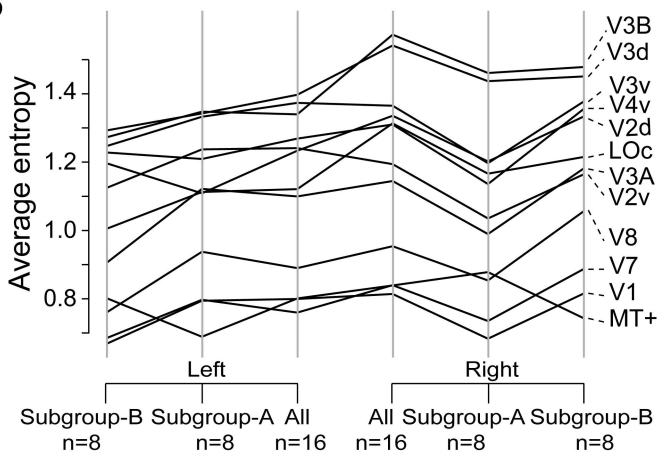


Figure 3.

A



B



C

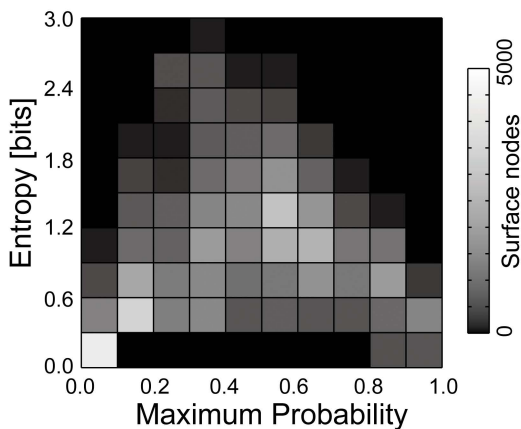
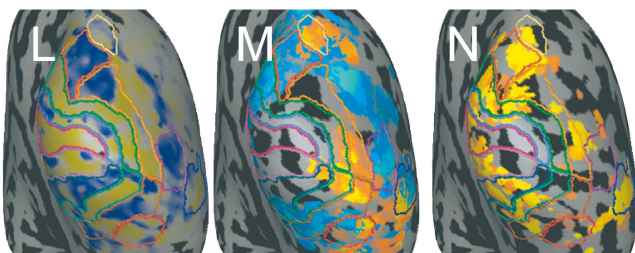
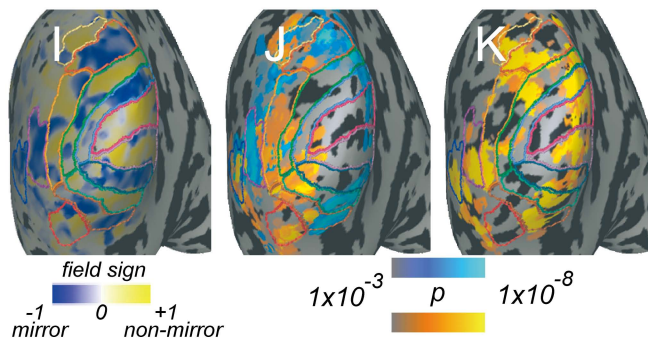
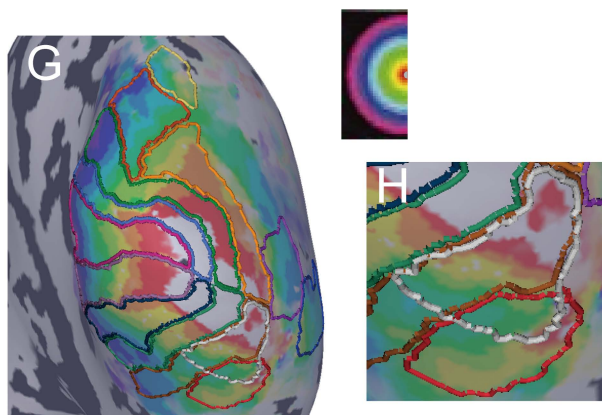
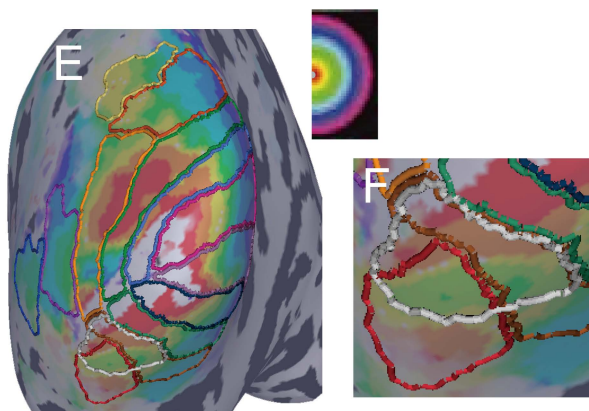
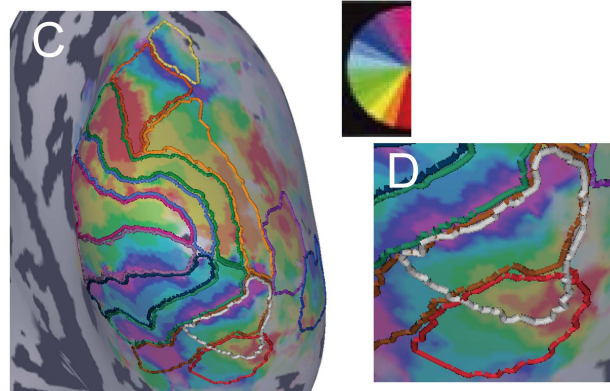
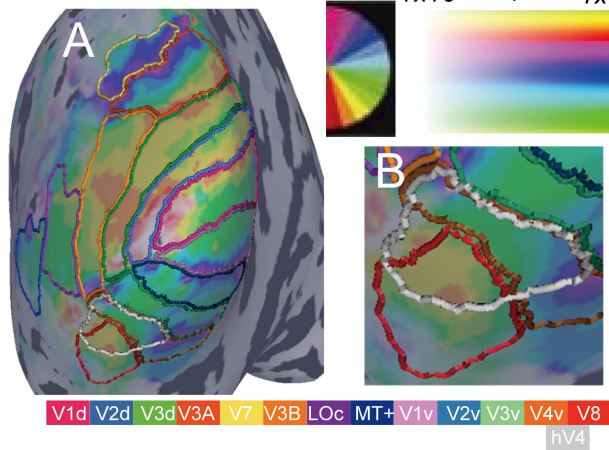
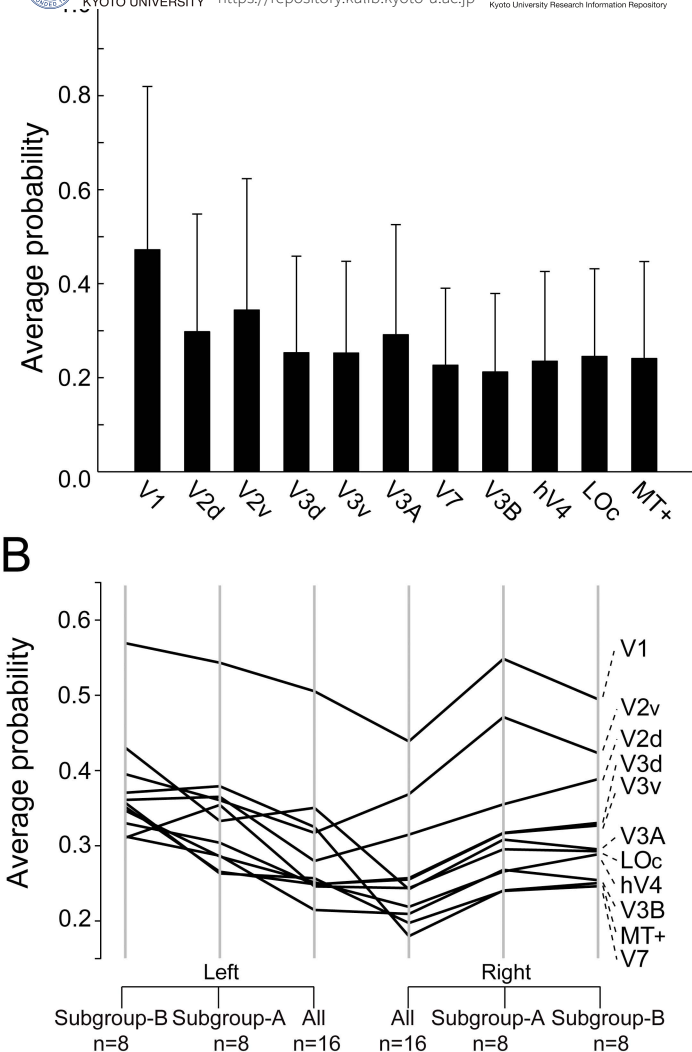


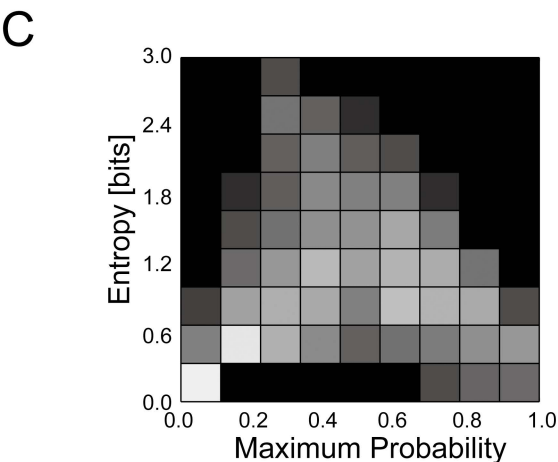
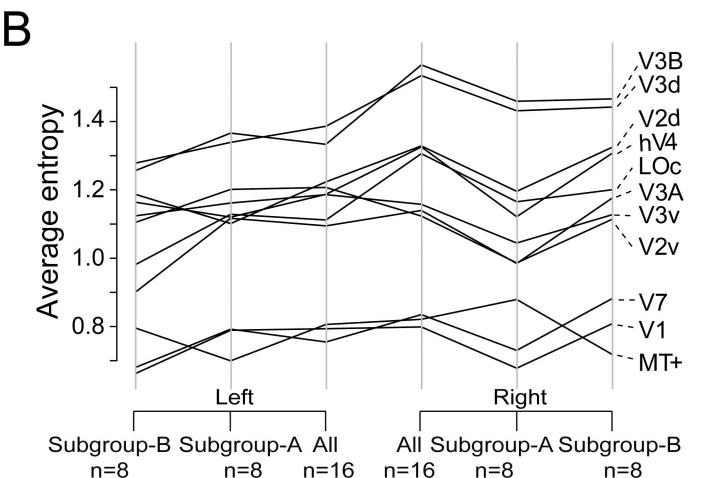
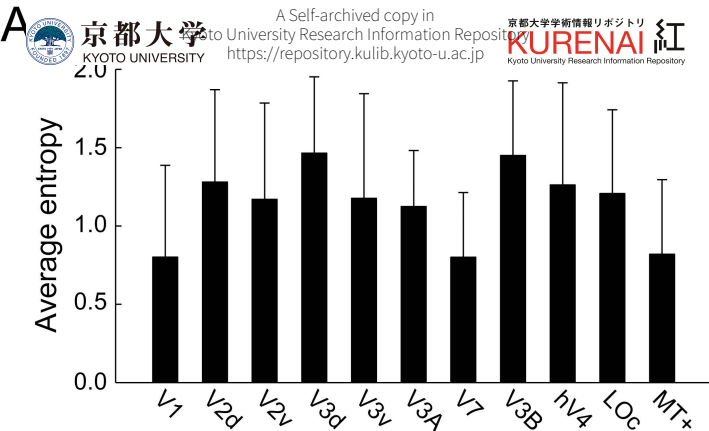
Figure 4.



Supplemental Figure S1.



Supplemental Figure S2.



Supplemental Figure S3.